Thermometry and Refrigeration in a Two-Component Mott Insulator of Ultracold Atoms

David M. Weld,* Patrick Medley,† Hirokazu Miyake, David E. Pritchard, and Wolfgang Ketterle

MIT-Harvard Center for Ultracold Atoms, Research Laboratory of Electronics,
and Department of Physics, Massachusetts Institute of Technology, Cambridge MA 02139

The two-component Mott insulator (2CMI) is a fundamental ingredient for experiments seeking to study spin physics using ultracold atoms in optical lattices. Recent experimental work has demonstrated that the 2CMI can be used for thermometry [1], and that its excitation spectrum enables a new cooling technique based on adiabatic reduction of an applied magnetic field gradient [2]. Comparison to theory is needed. We present results of calculations based on a model of the kinetic and spin degrees of freedom of a two-component Mott insulator in an inhomogeneous trapping potential at various temperatures and magnetic field gradients. We discuss higher-order corrections to spin gradient thermometry, and show that adiabatic reduction of the field gradient is capable of cooling below the Curie or Néel temperature of the spin ordered phases.

PACS numbers: 05.30.Jp, 37.10.Jk, 37.10.De, 75.30.Sg, 75.10.Jm, 07.20.Dt

The possibility of using ultracold lattice-trapped gases as general simulators of strongly interacting many-body systems has excited increasing interest in recent years [3– 5]. Spin hamiltonians are a natural candidate for quantum simulation, especially given the relevance of doped antiferromagnetic systems to the important open problem of high- T_c superconductivity [6]. The 2CMI is the starting point for simulation of electronic spin systems in lattices, and several interesting experiments have recently been performed in the 2CMI state [7, 8]. Spinexchange-stabilized magnetically ordered states are expected to exist in the 2CMI [9], and observation of these states and transitions between them would open up an exciting new field at the intersection of atomic and condensed matter physics. The main obstacle which has so far prevented the observation of spin-ordered states in the 2CMI is the very low temperature scale at which the spin ordering occurs. Quantum Monte Carlo calculations have predicted Curie and Néel temperatures on the order of 200 pK [10], which is a lower temperature than has ever been measured in any system. Clearly, new methods of thermometry and refrigeration are required. The recently demonstrated technique of spin gradient thermometry [1] should allow measurement of temperatures down to the spin exchange scale in the 2CMI. The related method of spin gradient demagnetization cooling is capable of cooling to the neighborhood of the critical temperature for spin ordering [2]. Together, these new techniques open a realistic prospect of preparing spin-ordered phases in the 2CMI. In order to compare experimental results with theory, we have developed a simple theoretical model of the 2CMI and used it to calculate the expected response of our experimental system to spin gradient thermometry and spin gradient demagnetization cooling.

Our treatment of the 2CMI is similar in approach to the studies of cooling in the one-component Mott insulator presented in Refs. [11] and [12], in that it is based on calculations of entropy-versus-temperature curves for various values of control parameters. Our model neglects the effects of tunneling, and treats each lattice site separately, yet it is capable of qualitatively reproducing observed cooling curves using only one fit parameter (the initial temperature) [2]. Our results thus complement the classical mean field and Monte Carlo analysis of Natu and Mueller [13], and are in qualitative agreement with their work.

The inputs to the calculation are the measured trap frequencies $(\omega_x, \omega_y, \omega_z)$, the total atom number N, and the applied magnetic field gradient $\nabla |\mathbf{B}|$ (along with various fixed parameters like the scattering lengths and magnetic moment of the atoms and the lattice constant). This allows direct comparison with experiment. The particular trap frequencies assumed here are $2\pi \times$ (40, 156, 141) Hz. We assume an atom number of 16000. These values were chosen because they are typical in our experiments. For a given temperature and magnetic field gradient, we calculate the energy of each spin configuration at each lattice site and use that to construct Boltzmann factors and a partition function. This allows us to calculate the entropy at every site in a 3D lattice; all lattice sites can then be summed to extract the total entropy as a function of temperature and field gradient. From this output one extracts simulated images, entropyversus-temperature curves, and the predicted response to demagnetization. The results of this calculation exhibit reasonable agreement with experimental data [2]. Fig. 1 shows some column-integrated spin images which the theory predicts, along with measured images.

Since the total magnetization is always fixed, the average value of the magnetic field is cancelled by a Lagrange multiplier and can be subtracted from the real field $\mathbf{B}(x)$. This allows us to write the field as $B_{\text{eff}} = \nabla |\mathbf{B}| \cdot \mathbf{x}_i$, where \mathbf{x}_i is the vector from the trap center to lattice site i projected along the direction of the magnetic field gradient.

^{*}Electronic address: dweld@mit.edu

 $^{^\}dagger \text{Present}$ address: Department of Physics, Stanford University, Stanford CA 94305

Note that $B_{\text{eff}} = 0$ at the trap center. If tunneling is neglected, then at a magnetic field gradient $\nabla |\mathbf{B}|$ the energy of a configuration with n_{\uparrow} up spins and n_{\downarrow} down spins at lattice site i is

$$E_{i}(n_{\uparrow}, n_{\downarrow}, \nabla |\mathbf{B}|) = p \cdot \nabla |\mathbf{B}| \cdot x_{i} \cdot (n_{\uparrow} - n_{\downarrow})$$

$$+ \frac{1}{2} \sum_{\sigma} U_{\sigma\sigma} n_{\sigma} (n_{\sigma} - 1) + U_{\uparrow\downarrow} n_{\uparrow} n_{\downarrow}$$

$$+ V_{i} \cdot (n_{\uparrow} + n_{\downarrow}) - \mu_{\uparrow} n_{\uparrow} - \mu_{\downarrow} n_{\downarrow}, (1)$$

where p is the amplitude of the effective magnetic moment of the atoms, $x_i = |x_i|$, $\sigma = \{\uparrow, \downarrow\}$, U_{ab} is the interaction energy between spin a and spin b, $V_i = (m/2)(\omega_x^2x_i^2 + \omega_y^2y_i^2 + \omega_z^2z_i^2)$ is the optical trapping potential at site i, y_i and z_i are the distances of site i from the trap center in the two directions transverse to the gradient, and μ_a is the chemical potential of spin a. The chemical potential is set by the requirement that the number of atoms of each spin be equal to half the total experimentally measured number.

Equation 1 can be used in the grand canonical ensemble to infer the thermal probability of different occupation numbers of the two spins. The partition function at lattice site i is $Z_i(\nabla |\mathbf{B}|) = \sum_{\{n_{\uparrow},n_{\downarrow}\}} \exp(-E_i(n_{\uparrow},n_{\downarrow},\nabla |\mathbf{B}|)/k_BT)$, where k_B is Boltzmann's constant, T is the temperature, and the summation is over all possible combinations of n_{\uparrow} and n_{\downarrow} (each combination is counted only once, due to indistinguishability of the atoms). The probability of having n_{\uparrow} up spins and n_{\downarrow} down spins at lattice site i is then

$$p_i(n_{\uparrow}, n_{\downarrow}, \nabla |\mathbf{B}|, T) = \frac{\exp\left(-E_i(n_{\uparrow}, n_{\downarrow}, \nabla |\mathbf{B}|)/k_B T\right)}{Z_i}$$
 (2)

and the resulting entropy at site i is

$$S_i(\nabla |\mathbf{B}|, T) = \sum_{\{n_{\uparrow}, n_{\downarrow}\}} -p_i \log p_i$$
 (3)

where the summation is performed in the same way as for the partition function. The only additional approximation needed is a truncation of the sums over spin configurations. For our experimental parameters, configurations corresponding to a total atom number per site greater than 4 can be safely neglected, and we have truncated the sums accordingly. This truncation is reminiscent of, but more general than, the particle-hole approximation [11, 12]. The site entropy S_i of Eq. 3 is summed over all lattice sites to extract the total entropy as a function of temperature for a given magnetic field gradient. Figure 2 shows the results of such a calculation for several values of the gradient.

It is instructive to compare the results of this calculation to those of the simple approximation which treats the spin and particle-hole degrees of freedom separately. In this approximation, the partition function for an individual lattice site i is assumed to factorize as $Z = Z_{\sigma} Z_0$, where $Z_{\sigma} = \sum_{\sigma} \exp(-\beta \boldsymbol{p}_{\sigma} \cdot \mathbf{B}(x_i))$, β is $1/k_B T$, \boldsymbol{p}_{σ} is the

magnetic moment of the spin σ , and Z_0 is the partition function of the particle-hole degrees of freedom (for which see [11, 12]). This simple treatment is generally valid for the case of one atom per lattice site. For occupation number n > 1, there are corrections which are captured by our more complete model. The first correction arises from a difference ΔU between the mean of the intra-spin interaction energies $\overline{U_{\sigma}}$ and the inter-spin interaction energy $U_{\uparrow\downarrow}$. $\Delta U/\overline{U_{\sigma}}$ is about 10^{-3} for ⁸⁷Rb. The leading correction changes the magnetic field gradient at the center of the sample B' to an effective gradient $B'(1+(n-1)\Delta U/k_BT)$. This becomes important at low temperatures, and destroys the factorizability of the partition function mentioned above. The second correction is due to indistinguishability of the atoms. This arises from the quantum mechanical fact that there are three (rather than four) possible spin states for a lattice site with two pseudospin-1/2 atoms. The size of both corrections is expected to be small, but in order to treat them fully we have developed the more general model described above, which does not assume unit occupation or that the partition function can be factorized into spin and kinetic terms. Detailed technical descriptions of spin

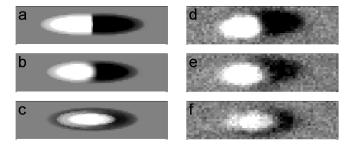


FIG. 1: Comparison of simulated and measured spin images. Simulated images are on the left. Magnetic field gradients and temperatures for simulated images are: **a:** 0.5 G/cm, 5 nK, **b:** 0.05 G/cm, 1 nK, and **c** 0.003 G/cm, 3 nK. Gradient and fitted temperature for each measured spin image **d-f** is close to the values for the simulated image in the same row. The expected curvature of the mixed-spin region is apparent in both simulated and real images at lower field gradients. See Fig. 3 for a comparison of the temperature extracted from this fit to the real modeled temperature.

gradient thermometry and spin gradient demagnetization cooling are presented in Refs. [1] and [2], respectively. Both techniques are based on the 2CMI in a magnetic field gradient. In both references, the two pseudospins are in fact the $|F=1,m_F=-1\rangle$ and $|F=2,m_F=-2\rangle$ hyperfine states of ⁸⁷Rb. Since the two components have different magnetic moments, the gradient pulls them towards opposite sides of the trap, creating two spin domains which remain in thermal contact. At zero temperature, there will be a zero-width boundary between the two domains, but at finite temperature a mixed region composed of spin excitations will be present. Under the assumption that $Z=Z_{\sigma}Z_{0}$, the mean spin $\langle s \rangle$ as a function of position, field gradient, and temperature has the

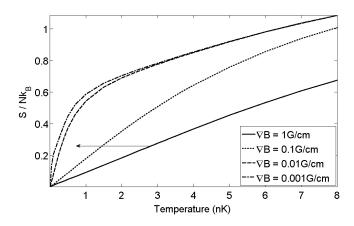


FIG. 2: Total entropy per particle versus temperature, at various gradients, for the experimental parameters described in the text. The arrow indicates the path followed during adiabatic spin gradient demagnetization cooling.

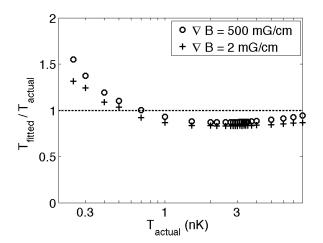


FIG. 3: Ratio between fitted temperature and actual temperature at two different gradients, assuming perfect imaging. This shows the effect of corrections due to indistinguishability and unequal scattering lengths. Finite imaging resolution will limit the ranges of temperature that can be measured with any given gradient, as discussed in Ref. [1].

simple form

$$\langle s \rangle = \tanh(-\beta \cdot \Delta \boldsymbol{p} \cdot \mathbf{B}(x_i)/2),$$
 (4)

where Δp is the difference between the magnetic moments of the two states. Spin gradient thermometry is based on the fact that at finite temperatures, the width of the boundary layer is proportional to the temperature and inversely proportional to the magnetic field gradient.

The spin profile of Eq. 4 is exact for a 2CMI with one particle per site. The model presented here can be used to investigate corrections to thermometry at higher filling. Figure 3 shows the temperature measured by fitting to Eq. 4 divided by the actual modeled temperature for two values of the gradient. The high-temperature

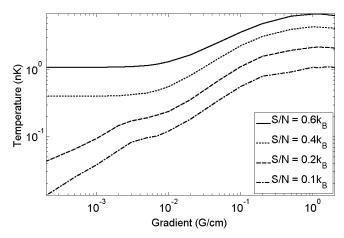


FIG. 4: Spin gradient demagnetization cooling. Predicted temperature versus final gradient, for several values of the total entropy.

correction is mainly due to indistinguishability of the atoms, and is only important for sites containing 2 or more atoms. Note that the fitted spin profile is integrated along both directions transverse to the gradient, so it includes contributions from all occupation number domains in the sample. Though this correction is conceptually important, it is not a large effect, and in no case does it change the measured temperature by more than 15% under our experimental conditions. The correction at low temperatures is partly due to the fact that the scattering lengths $U_{\uparrow\uparrow},\ U_{\downarrow\downarrow},$ and $U_{\uparrow\downarrow}$ are not all equal. The curvature of the mixed region which one would expect to result from unequal scattering lengths is observed in both simulated and measured data (see Fig. 1). This curvature arises from a buoyancy effect—the species with greater intraspin repulsion will preferentially populate the outer regions of the trap. This effect causes a fit to Eq. 4 to overestimate the temperature, since a curved boundary appears wider after integration along the directions perpendicular to the gradient. Another correction at low temperatures arises if the width of the mixed region becomes much less than one lattice constant. In this case both the model and the real physical spin system will not respond measurably to small changes in the gradient, and the measured temperature will overestimate the real temperature. These corrections need to be taken into account for precision temperature measurements at extreme temperatures and field gradients, but they do not alter the conclusions of Refs. [1] or [2].

Spin gradient demagnetization cooling is based on the fact that the entropy stored in the mixed region between the two spin domains increases with decreasing magnetic field gradient. If the change of the gradient is adiabatic, then the entropy which flows to the spin degrees of freedom must come from other degrees of freedom, and the sample's temperature is reduced. This is analogous to standard adiabatic demagnetization refrigera-

tion [14, 15], in which a paramagnetic material is placed in a strong magnetic field and allowed to come to thermal equilibrium, after which the field is slowly decreased, reducing the energy of spin flip excitations. Energy and entropy flow from other degrees of freedom into the spin degrees of freedom; the non-magnetic degrees of freedom are thus cooled.

However, although spin gradient demagnetization cooling was inspired by (and is locally similar to) adiabatic demagnetization refrigeration in condensed matter systems, there are important differences between the techniques. In addition to its applicability to latticetrapped atomic systems, spin gradient demagnetization cooling broadens and extends existing magnetic refrigeration techniques. For example, all prior realizations of demagnetization cooling (including one in an ultracold gas of chromium[16]) required spin-flips. Spin flip collisions in atomic gases are usually very slow, except for atoms with high magnetic moments such as chromium. However, spin gradient demagnetization cooling, because it uses a magnetic field gradient instead of a spatially homogeneous field, proceeds via spin transport in a system with fixed magnetization. On a practical level, it is also easier to achieve very small magnetic field gradients than very small magnetic fields. In our system, an energy resolution of $k_B \times 25$ picokelvin can be relatively easily achieved with a gradient of 1 milligauss/cm and an optical resolution of 5 μ m, while similar energy resolution in a homogeneous system would require control of the magnetic field at the microgauss level (assuming a magnetic moment of one Bohr magneton).

Entropy versus temperature curves such as those plotted in Fig. 2 can be used to calculate the response of the system to spin gradient demagnetization cooling. If the gradient is reduced perfectly adiabatically, the system will move horizontally as indicated by the arrow in Fig. 2, and the temperature will decrease. This behavior is plotted in Fig. 4 for several values of the total entropy (corresponding to different initial temperatures). These predictions can be used directly to fit experimental data, with the initial temperature being the only free parameter. Such fitting gives reasonable agreement with the data (see Ref. [2]).

For sufficiently low initial entropy, the spin degrees of freedom will contain all the entropy in the system when the gradient is adiabatically reduced by some factor. Further reduction of the gradient below this point is expected to linearly decrease the temperature of the system. This behavior is apparent in the lowest curve in Fig. 4. Conversely, if the initial entropy is too high, the spins will become fully disordered at some finite value of the gradient and will no longer be able to absorb entropy. Reduction of the gradient below this point will not change the temperature. This behavior is apparent in the upper curve in Fig. 4. If the gradient is sufficiently high, it can pull the two spin domains so far apart that the area where they overlap is decreased in size. This effect reduces the entropy capacity of the spin degrees of freedom at high gradients, and is the origin of the slight downturn in temperatures at the highest gradients in Fig. 4.

Magnetic field gradients of 1 mG/cm are well within the range of the experimentally achievable. Assuming reduction of the gradient from 2 G/cm to 1 mG/cm, our analysis predicts that samples with an initial entropy lower than about $0.3k_B$ can be cooled below the spin ordering temperature. Our model neglects spin correlations, so the lowest-temperature results plotted in Fig. 4 should be taken as evidence that reduction of the gradient is capable of cooling below the spin ordering temperature rather than a prediction of the dependence of temperature on gradient below the Curie or Nèel temperature.

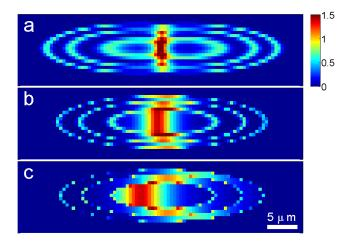


FIG. 5: Entropy distribution during spin gradient demagnetization cooling. The images are slices of the cloud through the center in the plane perpendicular to the imaging direction. All plots are at a total entropy per particle near 0.3 k_B , and are thus representative of the changing entropy distribution during isentropic demagnetization. Values of the gradient and temperature are as follows: a: $\nabla B = 0.5 \text{G/cm}, T = 3 \text{nK}$, b: $\nabla B = 0.1 \text{G/cm}, T = 1.5 \text{nK}$, c: $\nabla B = 0.02 \text{G/cm}, T = 0.5 \text{nK}$.

Figure 5 shows several images of the total entropy distribution at different final gradients during demagnetization. The pumping of entropy from the kinetic degrees of freedom to the spins is clearly visible, as is the curvature of the mixed-spin region due to nonzero ΔU .

We have presented results of calculations based on a theoretical model of the 2CMI and its response to a varying magnetic field gradient. Our results support the validity of the recently demonstrated techniques of spin gradient thermometry and spin gradient demagnetization cooling.

We thank Eugene Demler, Takuya Kitagawa, and David Pekker for useful and interesting discussions. H.M. acknowledges support from the NDSEG fellowship program. This work was supported by the NSF, through a MURI program, and under ARO Grant No. W911NF-07-1-0493 with funds from the DARPA OLE program. Correspondence and requests for materials should be addressed to D.M.W. (email: dweld@mit.edu).

- [1] D. M. Weld et al., Phys. Rev. Lett. 103, 245301 (2009).
- [2] P. Medley, D. M. Weld, H. Miyake, D. E. Pritchard, and W. Ketterle, Preprint at (http://arxiv.org/abs/1006.4674), 2010.
- [3] R. Feynman, International Journal of Theoretical Physics **21**, 467 (1982).
- [4] M. Lewenstein et al., Adv. Phys. 56, 243 (2007).
- [5] I. Bloch, J. Dalibard, and W. Zwerger, Rev. Mod. Phys. 80, 885 (2008).
- [6] P. A. Lee, N. Nagaosa, and X.-G. Wen, Rev. Mod. Phys. 78, 17 (2006).
- [7] R. Jordens, N. Strohmaier, K. Gunter, H. Moritz, and T. Esslinger, Nature 455, 204 (2008).
- [8] B. Gadway, D. Pertot, R. Reimann, and D. Schneble, Phys. Rev. Lett. 105, 045303 (2010).

- [9] L.-M. Duan, E. Demler, and M. D. Lukin, Phys. Rev. Lett. 91, 090402 (2003).
- [10] B. Capogrosso-Sansone, Ş. G. Söyler, N. V. Prokof'ev, and B. V. Svistunov, Phys. Rev. A 81, 053622 (2010).
- [11] T.-L. Ho and Q. Zhou, Phys. Rev. Lett. 99, 120404 (2007).
- [12] F. Gerbier, Phys. Rev. Lett. 99, 120405 (2007).
- [13] S. S. Natu and E. J. Mueller, Domain wall dynamics in a two-component Bose-Mott insulator, Preprint at (http://arxiv.org/abs/1005.3090), 2010.
- [14] W. F. Giauque, J. Amer. Chem. Soc. 49, 1864 (1927).
- [15] P. Debye, Ann. Phys. **386**, 1154 (1926).
- [16] M. Fattori et al., Nat. Phys. 2, 765 (2006).